

は発生しない。

### 3. 内耳イオン輸送に障害を持つ遺伝性難聴モデル

1999年、Minowaらはヒト非症候性遺伝性難聴因子Brn-4の遺伝子欠損マウスの作成に成功しこの機能解析を報告した(3)。この研究ではヒト非症候性遺伝性難聴であるDFN3の原因が有毛細胞ではなくラセン靭帯の線維細胞の変性にあることが初めて証明された。さらに内リンパ電位の形成に線維細胞が不可欠であるという新しい内耳の生理学的知見を明らかにした。この線維細胞やコルチ器の支持細胞等に強く発現し内耳イオン輸送体として重要な機能を担うのがCx26だが、2003年、Cx26遺伝子で初の遺伝子改変難聴モデルが開発されると(4)、コルチ器の形成不全・機能障害など新たな分子病態が明らかとなった(5,6)。最近、内耳特異的Cx26遺伝子欠損マウスが新規に開発され、有用な難聴モデル動物としてさらなる新規分子病態が明らかとなっている。

### 4. 蝸牛線維細胞を標的とした内耳細胞治療法

我々は新規治療法開発を目的として、蝸牛線維細胞のみに限局的な損傷を持つ聴覚障害モデルを開発し(7,8)、半規管からの外リンパ液還流法による骨髄間葉系幹細胞移植により聴力回復を促進させることに初めて成功した(9)。それまで幹細胞導入によって蝸牛内の損傷を修復し聴力回復に成功した例はなく、蝸牛線維細胞をターゲットとした骨髄間葉系幹細胞の移植法は今後有効な治療手段となり得ることが証明された。この方法では細胞移植後の拒絶反応も少なく他家移植としての有用性も示され、遺伝子変異細胞を正常細胞に置換する方法としても十分応用可能であることが示された。

### 5. 人工多能性幹(iPS)細胞からの内耳前駆細胞の樹立

2010年、iPS細胞、ES細胞からin vitroで内耳有毛細胞を作製する画期的技術がOshimaらにより発表され、作製された細胞が音の振動を感知できる有毛細胞特有のMET機能を有することが明らかとなった(10)。2012年にはES細胞からの内耳前駆細胞の新規作製法と実験動物への応用が報告された(11)。これにより内耳有毛細胞を体外で人工的に増殖・分化させることが可能であることが示された。新規手法をもとに様々な分化状態の内耳前駆細胞を樹立し、内耳移植に最も適した分化度の細胞を選抜することが可能であると考え

られる。これらの報告では、未分化細胞から外胚葉細胞、内耳前駆細胞へ、段階的に分化を進めており、これを応用して段階的に細胞の分離を行えば、難聴の原因となる全ての内耳構成細胞(有毛細胞、支持細胞、線維細胞、血管条細胞、ラセン神経節細胞)への分化能を持つ前駆細胞をin vitroにて作製し、標的細胞に応じた移植細胞を選抜することが可能となる。

我々の研究でもこの方法を応用することによりiPS細胞からMyosin7a発現とアクチン巨大絨毛を有する有毛細胞前駆細胞、コネキシン26発現細胞等が得られており、移植用幹細胞としての応用研究を進めている。

### 6. 新たな成体内耳幹細胞

最近、間葉系細胞への過剰ストレス負荷に耐性を持つ細胞から新たな多能性幹細胞が発見された(12)。同手法では遺伝子導入もなく安定的に増殖し間葉系幹細胞同様安全性が確保された幹細胞が得られると考えられる。我々はこの幹細胞樹立法を応用し成体内耳から初めて有毛細胞マーカーを発現する多能性幹細胞を樹立した。同細胞は一部に内耳有毛細胞のマーカーMyosin7aと共に細胞頂部に巨大絨毛様のアクチン重合を顕著に示す。この細胞は通常の間葉系幹細胞より増殖が二倍ほど遅く培養容器への強い接着を示すため、iPS細胞等から内耳前駆細胞への分化を誘導するためのフィーダー細胞としても適していた(未発表)。

### 7. 蝸牛標的組織への幹細胞の誘導

体外で内耳細胞を作製する技術は大きく進展しているが、作製された細胞を蝸牛組織へ直接的アプローチにて挿入することは蝸牛の構造上非常に困難である。Chenらの報告ではスナネズミのES細胞より分化誘導したラセン神経節細胞の前駆細胞を直接蝸牛軸へ注入し、神経細胞として機能させることに成功している(11)。蝸牛軸にガラス管等を挿入し細胞注入する導入方法は難易度が高く侵襲も高い。さらに齧歯類だけでも種間の解剖学的構造の差が大きく、人への臨床応用として安全性と有効性を確保することは困難なアプローチであると考えられる。感覚上皮である蝸牛有毛細胞とその支持細胞へのアプローチはさらに細胞構成が複雑なため困難が予想され、個体への生着と分化に成功した報告はいまだない。しかし適切な箇所に前駆細胞を挿入できる細胞誘導システムを開発すれば、低侵襲で安全かつ有効な技術が開発できると考えられる。筆者らは後半規管および外側半規管に小孔を開け、片側から微小チューブを挿入し細胞液で外リンパ液を還

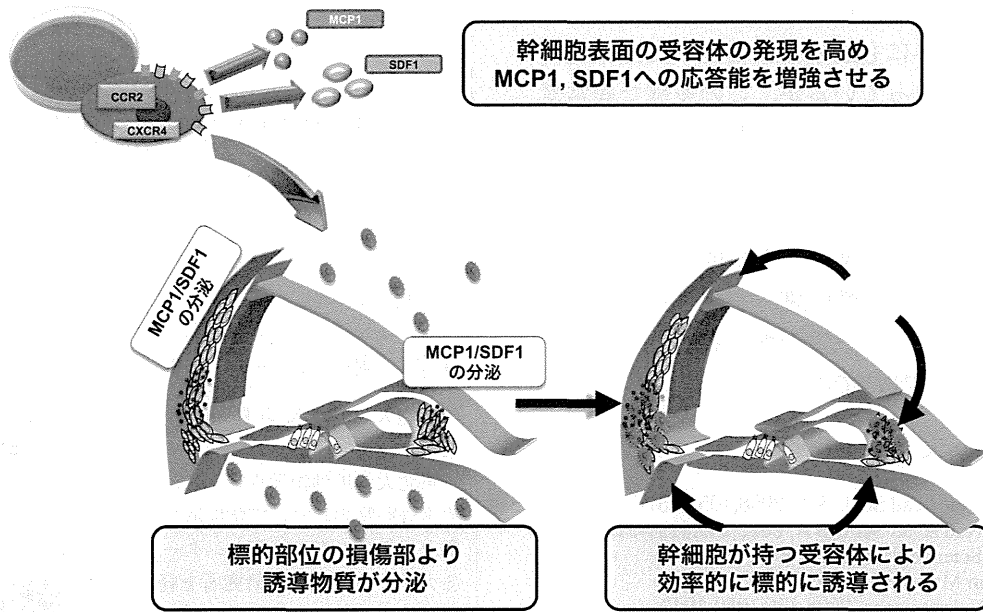


図1 幹細胞ホーミング機構を応用した内耳細胞治療法

培養シャーレ上で幹細胞（骨髄間葉系幹細胞等）にホーミング因子（MCP1, SDF1）を作用させそれらの受容体（CCR2, CXCR4）の発現を増強させる。移植前に薬物処置により蝸牛外側壁中心部にホーミング因子の発現を惹起させておき、外リンパ液中に上記前処置細胞を投与。この方法により蝸牛組織への幹細胞導入効率が大きく上昇する。

流する経半規管外リンパ液還流法を用いている(13)。同手法では手術による聴力低下はほとんど見られず、大量の細胞を外リンパ液中に導入することができるため、安全性を考慮した際の内耳細胞治療に適した投与方法であると思われる。我々は細胞液環流後に骨髄間葉系幹細胞の細胞塊を半規管の小孔に挿入することにより、術後のリンパ液の漏出を防ぎ、細胞生着にも良好な結果を得ている。

### 8. 内耳幹細胞ホーミング機構を応用した効率的細胞誘導法の開発

実用可能な内耳幹細胞治療法の開発のためには有毛細胞やその支持細胞および内リンパ液に接する血管条細胞、蝸牛線維細胞など適切な箇所に幹細胞を導入しその微小環境（niche, ニッチ, ニッシュ）に応じて分化させることが必要である。そのためには適切な幹細胞ホーミング（標的組織へ遊走し微小環境に生着）の分子機構を理解し応用することが重要であると考えられる。

マックスプランク研究所の報告では、心筋虚血後に骨髄由来間葉系幹細胞が癒痕層へ効率的にホーミングされるには走化性因子 MCP1, SDF1 とその受容体 CCR2, CXCR4 およびその下流において細胞遊走を制御している FROUNT による分子経路が重要な役割を担うことが明らかにされた(14)。

内耳におけるホーミングに関し、Tan らは音響障害を与えた蝸牛に多くの骨髄由来細胞が誘導され、走化性因子として SDF1 が機能していることを示している(15)。特に損傷後1週間で最も多くの骨髄由来細胞が蝸牛に誘導され、らせん靭帯の蝸牛線維細胞Ⅱ型周囲での SDF1 の発現と共に同部位への細胞誘導が示された。SDF1 が幹細胞ホーミング因子として組織損傷部への幹細胞誘導とその適応分化に関与するとの報告は多く(16)、内耳においても同因子がホーミングに重要な役割を担うと考えられる。

我々は上記のホーミング機構を応用し内耳での自然細胞誘導・修復機構を人為的に増強することにより、移植幹細胞の前処置によって MCP1, SDF1 の受容体である CCR2, CXCR4 の発現を効率的に上昇させることに成功した。同細胞を MCP1, SDF1 の発現を局所的に高めた蝸牛へ投与することにより蝸牛への幹細胞導入効率を約4倍に上昇させることが可能となった(図1)。さらに上記 Cx26 遺伝子欠損難聴モデルにおける Cx26 ギャップ結合を再構築させることに成功した(未発表)。同方法を最適化することにより大量の前駆細胞を内耳標的部位に導入し聴力回復に寄与できると考えられる。

### 9. おわりに

遺伝性難聴の治療においては人工内耳の有用性も報

告されているが、本来の聴覚機能を回復させる根本的治療法は未だ存在しない。遺伝性難聴の第一次的な原因細胞は有毛細胞以外にも蝸牛線維細胞や支持細胞であることが明らかとなっているが、この多様な異常変異細胞を修復するには新たな治療戦略として多能性幹細胞を用いた効率的細胞治療法の開発が必須であると考えられる。内耳における幹細胞ホーミング機構を理解し、自然細胞誘導・修復機構を人為的に分子制御することにより、様々な多能性幹細胞を蝸牛目的部位へ導入することが可能となり、安全性と有効性の高い新規細胞治療法の開発が期待できる。

## 文 献

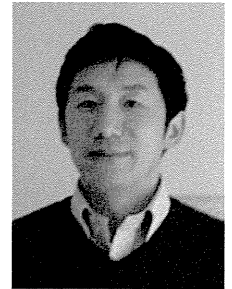
- 1) Nin F, et al. Proc Natl Acad Sci U S A. 2008;105:1751-1756.
- 2) Nin F, et al. Proc Natl Acad Sci U S A. 2012;109:9191-9196.
- 3) Minowa O, et al. Science. 1999;285:1408-1411.
- 4) Kudo T, et al. Hum Mol Genet. 2003;12:995-1004.
- 5) Inoshita A, et al. Neuroscience. 2008;156:1039-1047.
- 6) Minekawa A, et al. Neuroscience. 2009;164:1312-1319.
- 7) Hoya N, et al. Neuroreport. 2004;15:1597-1600.
- 8) Okamoto Y, et al. Audiol Neurootol. 2005;10:220-233.
- 9) Kamiya K, et al. Am J Pathol. 2007;171:214-226.
- 10) Oshima K, et al. Cell. 2010;141:704-716.
- 11) Chen W, et al. Nature. 2012;490:278-282.
- 12) Kuroda Y, et al. Proc Natl Acad Sci U S A. 2010;107:8639-8643.
- 13) Iguchi F, et al. Acta Otolaryngol Suppl. 2004;43-47.
- 14) Belema-Bedada F, et al. Cell Stem Cell. 2008;2:566-575.
- 15) Tan BT, et al. J Comp Neurol. 2008;509:167-179.
- 16) Hattori K, et al. Blood. 2001;97:3354-3360.

## 著者プロフィール

神谷 和作 (かみや かずさく)

順天堂大学 医学部 耳鼻咽喉科学講座、  
講師、博士 (獣医学)。

◇東北大応用動物学科卒、東大獣医学専攻実験動物学教室にて学位取得後、理研脳センター、東京医療センター、マイアミ大学、パスツール研究所を経て'08年現職。◇趣味：ラグビー。◇研究テーマ：内耳幹細胞治療法の開発。



## Gene Transfer Targeting Mouse Vestibule Using Adenovirus and Adeno-Associated Virus Vectors

\*Hiroko Okada, \*Takashi Iizuka, †Hideki Mochizuki, †Tomoko Nihira,  
\*Kazusaku Kamiya, \*Ayako Inoshita, \*Hiromi Kasagi, \*Misato Kasai,  
and \*Katsuhisa Ikeda

\*Department of Otorhinolaryngology, Juntendo University Faculty of Medicine, Tokyo; and †Department of Neurology, Kitasato University School of Medicine, Sagami-hara, Kanagawa, Japan

**Hypothesis:** The present study assessed how to inject a gene into the mouse vestibule and which is the optimum gene to the mouse vestibule adenovirus (AdV) vector or adeno-associated virus (AAV) vector.

**Background:** Loss of vestibular hair cell is seen in various balance disorder diseases. There have been some reports concerning gene delivery to the mouse vestibule in recent years. To effectively induce transgene expression at the vestibule, we assessed the efficiency of inoculating the mouse inner ear using various methods.

**Methods:** We employed an AdV- and AAV-carrying green fluorescent protein using a semicircular canal approach (via a canalostomy) and round window approach.

**Results:** AAV injection via canalostomy induced gene expression at the hair cells, supporting cells, and fibrocytes at the vestibular organs without auditory or balance dysfunction, suggesting it was the most suitable transfection method. This method is thus considered to be a promising strategy to prevent balance dysfunction.

**Conclusion:** AAV injection via canalostomy to the vestibule is the noninvasive and highly efficient transfection method, and this study may have the potential to repair balance disorders in human in the future. **Key Words:** Gene therapy—Vestibule—Virus vector.

*Otol Neurotol* 33:655–659, 2012.

The loss of vestibular cells is seen in various balance disorders such as aging, aminoglycoside toxicity, and herpes zoster otitis (1–3), and it is known that many children with congenital deafness have a disorder in the vestibular function. In such cases, bilateral vestibular loss results in permanent chronic balance dysfunction. The vestibular system is an especially important target for hair cell regeneration because no clinical treatments are currently available for patients that have lost all vestibular function. Animal models with genetic balance disorder were discovered and generated mostly in mouse, such as shaker-1 or waltzer mice, a mouse model for Usher syndrome. There have many reports about gene delivery to the mouse inner ear in recent years. Several investigators reported that gene transfer using adenovirus-based vectors results in vestibular hair cell regeneration, recovery of balance function (4), and

vestibular hair cell preservation from aminoglycosides (5). However, it is difficult to use adenoviruses because they would be used for only short-term treatment (6). Therefore, we compared the effect of adenovirus (AdV) vectors with recombinant adeno-associated viral (rAAV) vectors, which has the advantages in causing long-term gene expression compared with AdV (7). Moreover, we assessed how to inject a gene into the mouse inner ear. Three main routes of gene delivery are possible, namely, scala media approaches (via a cochleostomy), semicircular canal approaches (via a canalostomy), and round window approaches (8,9). Hearing loss by the method of cochleostomy has been reported in some studies (9,10). Thus, in this study, the delivery of AdV and rAAV via semicircular canal or round window was investigated to elucidate the implications for hearing and balance function and cellular specificity of the transgene expression in the mouse vestibule.

### MATERIALS AND METHODS

#### Animals

Healthy C57BL/6 male mice were used at p14. All experimental protocols were approved by the Institutional Animal

Address correspondence and reprint requests to Takashi Iizuka, M.D., Ph.D., Department of Otorhinolaryngology, Juntendo University Faculty of Medicine, 2-1-1 Hongo, Bunkyo-ku, Tokyo 113-8421, Japan; E-mail: t-iizuka@juntendo.ac.jp

The sources of any support for the work in the form of grants are none. The authors disclose no conflicts of interest.

Care and Use Committee at Juntendo University and were conducted in accordance with the U.S. National Institutes of Health Guide for the Care and Use of Laboratory Animals.

### Vectors

A replication-deficient vector (human AdV, serotype 5) was used to encode the green fluorescent protein (GFP) driven by the cytomegalovirus (CMV) promoter. The virus was designated AD5.CMV-GFP ( $3 \times 10^{11}$  pfu/ml). The E1 and E3 regions were deleted. The vectors were purchased from Arist Company, Osaka, Japan. Viral suspensions in 10 mM Tris-HCl, pH 7.5, 1 mM MgCl<sub>2</sub>, and 10% glycerol were kept at  $-80^{\circ}\text{C}$  until thawed for use.

The plasmid DNA pAAV-MCS (CMV promoter; Stratagene, La Jolla, CA, USA) carrying the GFP gene was constructed as reported previously (11). The plasmid DNA pAAV-GFP was cotransfected with plasmids pHelper and Pack2/1 into HEK-293 cells using the standard calcium phosphate method (12). After 48 hours, the cells were harvested, and crude rAAV vector (serotype 1) solutions were obtained by repeated freeze-thaw cycles. After ammonium sulfate precipitation, the virus particles were dissolved in phosphate-buffered saline (PBS) and applied to an OptiSeal centrifugation tube (Beckman Coulter, Fullerton, CA, USA). After overlaying with an OptiPrep solution (Axis-Shield PoC, Oslo, Norway), the tube was processed with a Gradient Master (BioCpmp Instruments, Frederickton, NB, Canada) to prepare the gradient layer of the OptiPrep. The tube was then ultracentrifuged at 13,000 r.p.m. for 18.5 hours. The fractions containing high-titer rAAV vectors were collected and used for injection into animals. The number of rAAV genome copies was semiquantified using polymerase chain reaction (PCR) within the CMV promoter region using primers 5'-GACGTCAATAATGACGTATG-3'

and 5'-GGTAATAGCGATGACTAATACG-3'. The final titer was  $1.4 \times 10^{13}$  vp/ml.

To compare the infectious efficiency of the 2 vectors, the same volume (0.5  $\mu\text{l}$ ) of AdV-GFP and AAV-GFP from the same lots used in the present cochlear injection were administered in 60-mm dish with confluent HEK293 cells and observed in 24 hours after the infection.

### Surgical Procedures

C57BL/6 male mice were anesthetized with ketamine (100 mg/kg) and xylazine (4 mg/kg) by intraperitoneal injection. Glass capillaries (Drummond Scientific, Broomall, PA, USA) were drawn with a PB-7 pipette puller (Narishige, Tokyo, Japan) to achieve an approximately 10- $\mu\text{m}$  outer tip diameter. A polyethylene tube (Atom Medical, Saitama, Japan) was connected to the glass micropipette. After making a left postauricular incision, the vector was injected following either of the 2 routes.

**Round window approach:** for injection via the round window, the left otic bulla was opened, and the glass micropipette was inserted into the round window up to the scala tympani, and the vectors were injected using the micropipette. The injection volume of the viral vector was regulated to approximately 0.1  $\mu\text{l}/\text{min}$  for 5 minutes using a syringe connected to the polyethylene tube. To allow the vector to spread throughout and stabilize in the inner ear, the glass micropipette was left in place for 1 minute after the injection. The opening region of the otic bulla was sealed with connective tissue.

**Semicircular canal approach:** for injection via canalostomy, after anesthesia, the posterior and lateral semicircular canals were identified, and a small hole was made in each canal. Next, the glass pipette was inserted into the hole of the posterior semicircular canal, and the vectors were injected in the same manner as with the round window approach.

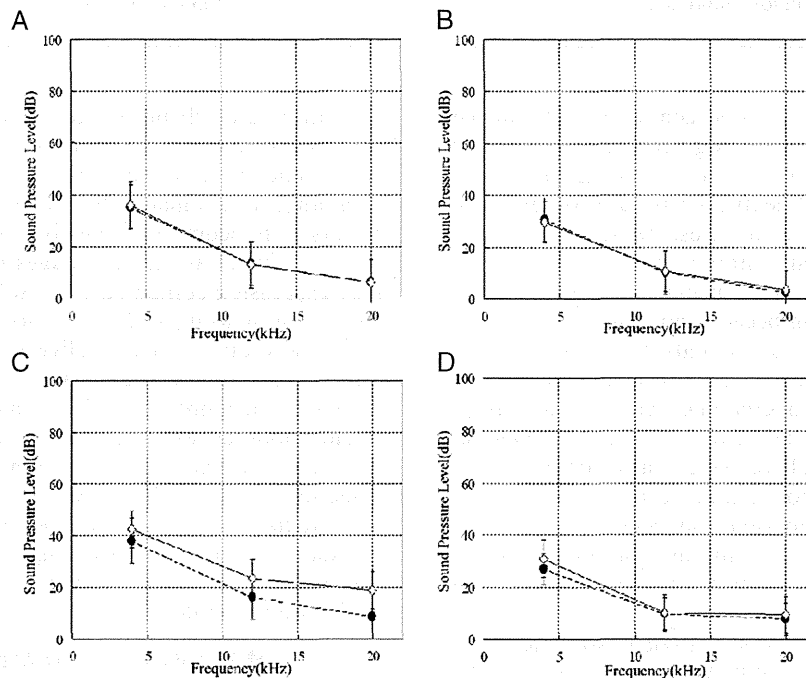


**FIG. 1.** Hearing results at 14 days after virus vector injection. The ABR thresholds of postoperation (*hollow squares*) did not differ from the preoperative results (*solid circles*) of AAV injection via the round window (*A*) and via canalostomy (*B*) and the AdV injection via canalostomy (*D*). At AdV injection via the round window, statistical significance was seen at 20 kHz (*C*). ( $*p < 0.05$ ).

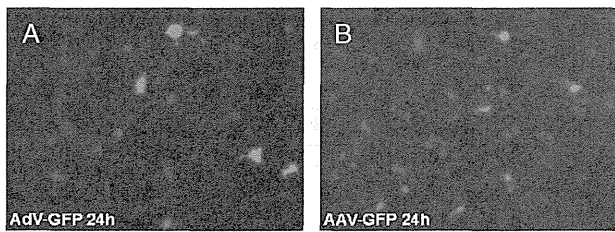


**FIG. 2.** The same volume (0.5  $\mu$ l) of AdV-GFP (A) and AAV-GFP (B) from the same lots used in the present cochlear injection were administrated in 60-mm dish with confluent HEK293 cells and observed in 24 hours after the infection. GFP signals showed approximately same infection rates. Images were represented by GFP fluorescent overlaid on phase contrast image.

### Measurements of Auditory Brainstem Response

To assess the safety of the gene transfer strategy, we assessed the auditory brainstem response (ABR) preoperatively and 14 days after the operation at the virus-injected ear (left side). ABR measurements were performed as previously reported in our laboratory (13). Thresholds were determined for frequencies of 4, 12, and 20 kHz from a set of responses at various intensities with 5-dB intervals, and the electrical signals were more than 512 repetitions.

### Assessment of Vestibular Function

We assessed the vestibular function by observation of the head tilt, reaching response, and swimming test at 14 days after operation. For the reaching response, the mouse was held by the tail above a flat surface, and it was noted whether the forepaws were stretched out to make contact with the surface. For the swimming test, the animals were placed in a container filled with 30 cm of comfortably warm water for no longer than 60 seconds.

### Sample Preparation, Histology, and Immunohistochemical Analysis

At 14 days after injection, the mice were anesthetized and perfused intracardially with PBS, followed by 4% paraformaldehyde (PFA) in phosphate buffer. The whole inner ear structures were excised and fixed with PFA and then decalcified in 0.12M ethylenediamine tetra-acetic acid. Specimens were cryoprotected in 30% sucrose in PBS, embedded, frozen, and sectioned at 10  $\mu$ m. Immunofluorescence analysis was performed as previously reported (10) using anti-GFP antibodies, rhodamine-phalloidin, and 4'6-diamidino-2-phenylindole (DAPI). Images of sections were captured with a Carl Zeiss Axioplan 2 microscope (Carl Zeiss, Oberkochen, Germany), KEYENCE VB-G25 (KEYENCE, Osaka, Japan), and Carl Zeiss LSM510 META (Carl Zeiss, Oberkochen, Germany).

### Data Analysis

Statistical analyses were performed using Student's *t*-test for the ABR data in StatMate IV for Windows. Differences were considered to be significant if  $p < 0.05$ .

## RESULTS

### Functional Evaluation

The ABR thresholds at frequencies of 4, 12, and 20 kHz are shown in Figure 1. The ABR thresholds 14 days

after virus vector injection did not differ from the preoperative results in the rAAV injection (Fig. 1, A and B) and AdV injection via canalostomy groups (Fig. 1D). With AdV injection via the round window (Fig. 1C), the ABR threshold at 20 kHz was significantly elevated postoperatively (Fig. 1C) ( $*p < 0.05$ ). For vehicle control, a sham treatment using sterile normal saline through the round window or semicircular canal had been done without hearing loss (data not shown).

No abnormalities were observed in the vestibular functional tests (head tilt, reaching response, and swimming test) in any animal 14 days after the operation.

### The Infectious Efficiency of the 2 Vectors

GFP signals showed approximately same infection rates, suggesting that these 2 lots of virus had the same titer level. Images were represented by GFP fluorescent overlaid on phase contrast image (Fig. 2).

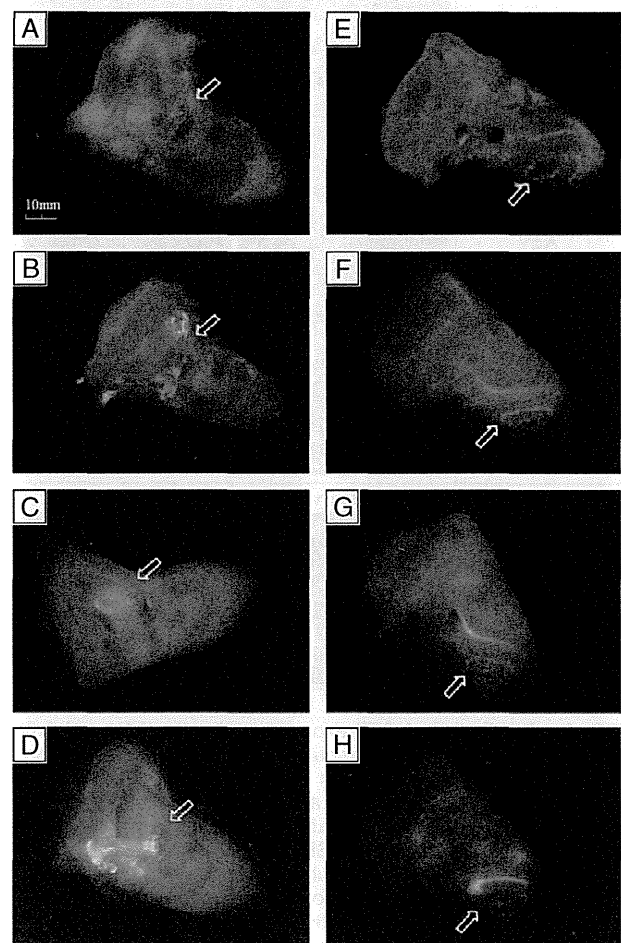


**FIG. 3.** Photomicrographs of whole inner ear images after dissection with a fluorescence stereoscopic microscope. AAV injected inner ear via the round window (A, E), AAV injected via canalostomy (B, F), AdV injected via the round window (C, G), and AdV injected via canalostomy (D, H).

### Whole Inner Ear Observation

To confirm the infection of the inner ear, we observed the whole inner ear without staining using a fluorescence stereoscopic microscope. GFP signals were observed in the vestibular organs (Fig. 3, A–D) and the cochlea (Fig. 3, E–H) with all the methods.

### Expression of GFP

We observed the immunostained frozen sections of the vestibular organs with a fluorescence microscope to

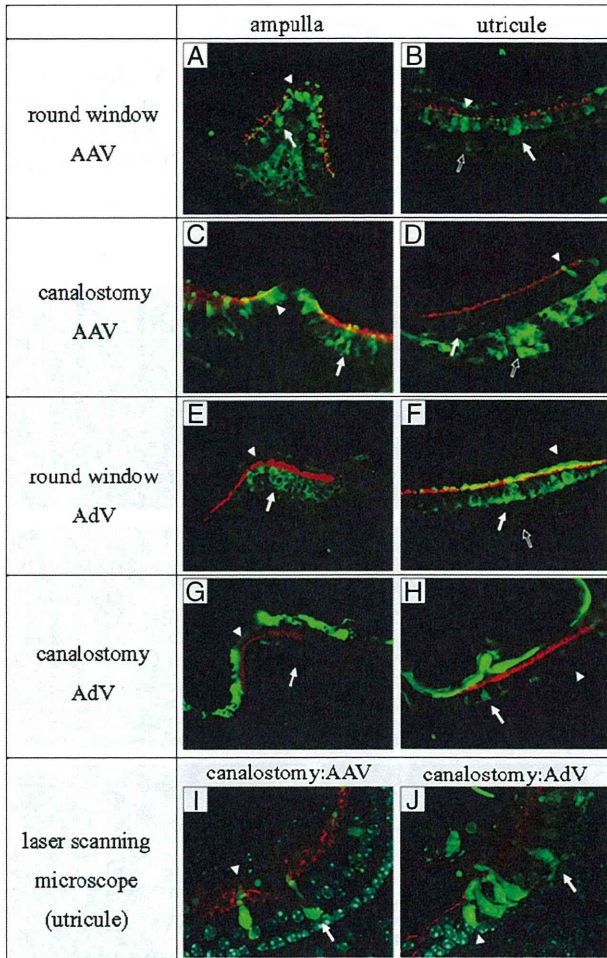


**FIG. 4.** Distribution of GFP expression after the AAV and AdV injection. *A, C, E, and G* are ampulla and *B, D, F, and H* are utricule. GFP expression could be seen in vestibular hair cells (arrowheads), supporting cells (white arrows) and fibrocytes (outlined arrows) in the inner ear tissue after AAV injection via the round window (*A, B*). Expression of GFP also was seen in hair cells and supporting cells in the ampulla and utricule, and higher GFP expression observed in the fibrocytes compared with the other methods (*C, D*). With AdV injection via the round window (*E, F*) and canalostomy (*G, H*), transgene expression is detected in the ampulla and utricule, including the hair cells and supporting cells. *I* and *J* are the images using a laser scanning microscope. GFP expressions were observed in vestibular hair cells (arrowheads) and supporting cells (white arrows) with the methods of AAV injection via canalostomy (*I*) and AdV injection via canalostomy (*J*).

**TABLE 1.** Expression of green fluorescent protein in the vestibular organ

	Ampulla		Utricule		Fibrocyte
	HC	SC	HC	SC	
AAV-RW injection	++	+	++	+	+
AAV-canalostomy	++	++	+	+	++
AdV-RW injection	+	+	+	+	+
AdV-canalostomy	+	+	+	+	+

The number of infected cells in one section is 0 (–), 1–5 (+), and 6–10 (++)

HC indicates hair cell; RW injection, transgene via the round window membrane; SC, supporting cell.

assess the cellular specificity of the transgene expression of the virus vectors and the numbers of infected cells. No pathologic changes were observed in the vestibular organs. GFP expression could be seen in vestibular hair cells (arrowheads), supporting cells (white arrows), and fibrocytes (outlined arrows) in the inner ear tissue after rAAV injection via the round window ( $n = 4$ ; Fig. 4, *A* and *B*). After rAAV injection via canalostomy, the expression of GFP also was seen in hair cells and supporting cells in the ampulla and utricule, and higher GFP expression was observed in the fibrocytes as compared with the other methods ( $n = 6$ ; Fig. 4, *C* and *D*). After AdV injection via the round window ( $n = 4$ ; Fig. 4, *E* and *F*) and canalostomy ( $n = 5$ ; Fig. 4, *G* and *H*), transgene expression was detected in the ampulla and utricule, corresponding to the hair cells and supporting cells.

For the purpose of identifying GFP-expressing cells, the sections were observed and image-stacked using a confocal laser scanning microscope. After rAAV injection via canalostomy (Fig. 4*I*) and AdV injection via canalostomy (Fig. 4*J*), the expression of GFP occurred in supporting cells, organizing a single layer, and hair cells in the shape of flask or column form.

### Comparison of the Number of the Infected Cells by Injection Method

We assessed the cellular specificity by counting the numbers of cells expressing GFP (Table 1). In the hair cells in the ampulla, there were more transfected cells by rAAV injection than by AdV injection. In the supporting cells of the ampulla, the rAAV injection by canalostomy showed the most cells with GFP expression. In the utricule, rAAV injection via the round window showed the most cells with GFP expression of all methods. For vestibular fibrocytes, rAAV injection by canalostomy showed the most transfected cells.

### DISCUSSION

The present study is the first report comparing the gene expression at the vestibule between round window and canalostomy approaches. Most of our methods were shown to be safe in terms of hearing function and vestibular function because no ABR threshold shift or balance

abnormality was observed in our study. Especially, the strategy to inject the virus in the ear by canalostomy has no risk of causing hearing impairment because of the surgical manipulation. In the comparison of the number of transfected cells by the injection methods, rAAV injection by canalostomy was demonstrated to have the most and was safe for transgene infection into the vestibular hair cells and other functional cells in the vestibule.

At present, AdV vectors are commonly used in animal experiments of gene therapy for the inner ear. Staecker et al. (4) demonstrated that math1 gene transfer using AdV results in vestibular hair cell regeneration and recovery of the balance function. Moreover, Pfannenstiel et al. (5) demonstrated that bcl-2 gene transfer using AdV preserved vestibular hair cells after exposure to aminoglycosides. The expression time of AAV may be more useful for therapeutics requiring long time expression, whereas AdV would be used for short-term treatments (6).

Kawamoto et al. (9) reported that no significant ABR threshold shift appeared after the injection of AdV vectors into the mouse inner ear. On the other hand, our study showed that the injection of AdV vectors via the round window significantly elevated the ABR threshold postoperatively at 20 kHz. AdV vectors may cause an inflammatory response in the inner ear because higher titers of AdV and rAAV were used in the present study than in the reports by Kawamoto et al.

Because the titer of rAAV was different from that of AdV, we could not compare the efficiency of AdV with AAV. Although the ABR threshold was significantly elevated after the AdV injection via the round window, it was not elevated after the AAV injection. In addition, the infected hair cells, supporting cells and fibrocytes of the ampulla by AAV injection were greater in number than those by AdV. Thus, rAAV vectors are more suitable than AdV for the purpose of gene therapy to the vestibule.

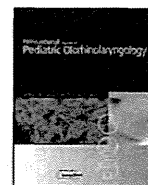
With AdV injection via a canalostomy, transgene expression was reported to be limited to the perilymphatic space (9). In our study, both AdV and rAAV injection via canalostomy showed transgene expression in vestibular hair cells and supporting cells. Our results differ from those of a previous study (9) and may be explained by the use of the fine glass capillary, which maintains the structure and function of the membranous labyrinth.

Our noninvasive and highly efficient transfection method could enable transgene infection into the vestibule and may have the potential to repair balance disorders in human in the future.

## REFERENCES

1. Tsuji K, Velazquez-Villasenor L, Rauch SD, Glynn RJ, Wall C 3rd, Merchant SN. Temporal bone studies of the human peripheral vestibular system. Meniere's disease. *Ann Otol Rhinol Laryngol Suppl* 2000;181:26-31.
2. Tsuji K, Velazquez-Villasenor L, Rauch SD, Glynn RJ, Wall C 3rd, Merchant SN. Temporal bone studies of the human peripheral vestibular system. Aminoglycoside ototoxicity. *Ann Otol Rhinol Laryngol Suppl* 2000;181:20-5.
3. Proctor L, Perlman H, Lindsay J, Matz G. Acute vestibular paralysis in herpes zoster oticus. *Ann Otol Rhinol Laryngol* 1979;88:303-10.
4. Staecker H, Praetorius M, Baker K, Brough DE. Vestibular hair cell regeneration and restoration of balance function induced by math1 gene transfer. *Otol Neurotol* 2007;28:223-31.
5. Pfannenstiel SC, Praetorius M, Plinkert PK, Brough DE, Staecker H. Bcl-2 gene therapy prevents aminoglycoside-induced degeneration of auditory and vestibular hair cells. *Audiol Neurootol* 2009;14:254-66.
6. Berkner KL. Expression of heterologous sequences in adenoviral vectors. *Curr Top Microbiol Immunol* 1992;158:39-66.
7. Kaplitt MG, Xiao X, Samulski RJ, et al. Long-term gene transfer in porcine myocardium after coronary infusion of an adeno-associated virus vector. *Ann Thorac Surg* 1996;62:1669-76.
8. Lalwani AK, Walsh BJ, Carvalho GJ, Muzyczka N, Mhatre AN. Expression of adeno-associated virus integrated transgene within the mammalian vestibular organs. *Am J Otol* 1998;19:390-5.
9. Kawamoto K, Oh SH, Kanzaki S, Brown N, Raphael Y. The functional and structural outcome of inner ear gene transfer via the vestibular and cochlear fluids in mice. *Mol Ther* 2001;4:575-85.
10. Iizuka T, Kanzaki S, Mochizuki H, et al. Noninvasive in vivo delivery of transgene via adeno-associated virus into supporting cells of the neonatal mouse cochlea. *Hum Gene Ther* 2008;19:384-90.
11. Yamada M, Iwatsubo T, Mizuno Y, Mochizuki H. Overexpression of alpha-synuclein in rat substantia nigra results in loss of dopaminergic neurons, phosphorylation of alpha-synuclein and activation of caspase-9: resemblance to pathogenetic changes in Parkinson's disease. *J Neurochem* 2004;91:451-61.
12. Sambrook JRD, Russel DW. Calcium-phosphate-mediated transfection of eukaryotic cells with plasmid DNAs. In: Irwin N, Janssen KA, eds. *Molecular Cloning: A Laboratory Manual*. New York, NY: Cold Spring Harbor Laboratory Press, 2001:16.14-16.20.
13. Inoshita A, Iizuka T, Okamura HO, et al. Postnatal development of the organ of Corti in dominant-negative Gjb2 transgenic mice. *Neuroscience* 2008;156:1039-47.





## Prevalence of *GJB2* causing recessive profound non-syndromic deafness in Japanese children

Chieri Hayashi<sup>a,\*</sup>, Manabu Funayama<sup>b</sup>, Yuanzhe Li<sup>c</sup>, Kazusaku Kamiya<sup>a</sup>, Atsushi Kawano<sup>d</sup>, Mamoru Suzuki<sup>d</sup>, Nobutaka Hattori<sup>b,c</sup>, Katsuhisa Ikeda<sup>a</sup>

<sup>a</sup> Department of Otorhinolaryngology, Juntendo University School of Medicine, 2-1-1 Hongo, Bunkyo-ku, Tokyo 113-8421, Japan

<sup>b</sup> Research Institute for Diseases of Old Age, Juntendo University School of Medicine, Japan

<sup>c</sup> Department of Neurology, Juntendo University School of Medicine, Japan

<sup>d</sup> Department of Otorhinolaryngology, Tokyo Medical University School of Medicine, Tokyo, Japan

### ARTICLE INFO

#### Article history:

Received 14 June 2010

Received in revised form 18 October 2010

Accepted 2 November 2010

Available online 26 November 2010

#### Keywords:

Congenital deafness  
Cochlear implantation  
Japanese children  
p.P225L  
Connexin 26  
*GJB2*

### ABSTRACT

**Objective:** *GJB2* (gap junction protein, beta 2, 26 kDa: connexin 26) is a gap junction protein gene that has been implicated in many cases of autosomal recessive non-syndromic deafness. Point and deletion mutations in *GJB2* are the most frequent cause of non-syndromic deafness across racial groups. To clarify the relation between profound non-syndromic deafness and *GJB2* mutation in Japanese children, we performed genetic testing for *GJB2*.

**Methods:** We conducted mutation screening employing PCR and direct sequencing for *GJB2* in 126 children who had undergone cochlear implantation with congenital deafness.

**Results:** We detected 10 mutations, including two unreported mutations (p.R32S and p.P225L) in *GJB2*. We identified the highest-frequency mutation (c.235delC: 44.8%) and other nonsense or truncating mutations, as in previous studies. However, in our research, p.R143W, which is one of the missense mutations, may also show an important correlation with severe deafness.

**Conclusion:** Our results suggest that the frequencies of mutations in *GJB2* and *GJB6* deletions differ among cohorts. Thus, our report is an important study of *GJB2* in Japanese children with profound non-syndromic deafness.

© 2010 Elsevier Ireland Ltd. All rights reserved.

### 1. Introduction

People with any degree of sensory impairment may encounter problems such as discrimination within the education system or when looking for work, and a reduced life expectancy. Sensorineural hearing loss (SNHL) is the most common sensory impairment in developed societies [1,2], where one child in 1000 presents at birth with severe or profound deafness [3].

Recent advances in human genetics have indicated that more than half of congenital SNHL cases involve a genetic factor [4]. In 75–80% of genetic cases, SNHL is the result of autosomal recessive inheritance, and both parents have normal hearing [5]. Mutations of *GJB2* are the most frequent cause of autosomal recessive non-syndromic deafness. Indeed, previous studies have shown that *GJB2* mutations account for up to 50% of non-syndromic deafness cases [6]. Hearing-impaired subjects with biallelic *GJB2* mutations range widely but most commonly follow a severe to profound and non-progressive pattern [7–9]. About 100 different *GJB2* muta-

tions have been reported globally [the Connexin-Deafness homepage: <http://davinci.crg.es/deafness/>], and these mutations show a relatively high local dependence (founder effect). A high prevalence of c.35delG has been found among Caucasians; c.235delC among Eastern Asians, including Japanese [10–13]; c.167delT among Ashkenazi Jews [14]; p.R143W among certain Africans [15]; and p.W24X among Indians [16,17] and European Gypsies [18–20]. Some recent reports have indicated a genotype-phenotype correlation: children with two truncating mutations, such as c.35delG or c.235delC, are profoundly deaf, while children with a truncating and missense mutation, or two missense mutations, show better hearing [9,21,22]. Since improved speech performance after cochlear implantation in early childhood is usually observed in hearing-impaired subjects with *GJB2* mutations [23], the genetic testing of newborn babies will provide useful prognostic information when selecting appropriate treatment for such children.

In the present study, to clarify the frequency and genotype-phenotype correlation of *GJB2* mutations in children with profound non-syndromic deafness, we performed genetic testing for *GJB2* mutations involving 119 Japanese children who had undergone cochlear implantation with congenital deafness.

\* Corresponding author. Tel.: +81 3 5802 1229; fax: +81 3 5840 7103.  
E-mail address: [chieri-h@juntendo.ac.jp](mailto:chieri-h@juntendo.ac.jp) (C. Hayashi).

## 2. Materials and methods

### 2.1. Subjects

We enrolled 119 Japanese children, who were unrelated to each other, with non-syndromic deafness for genetic analysis. Of these, 107 were sporadic cases (with only one affected individual in the family); the remaining 12 patients were autosomal recessive cases (with normal hearing parents and at least two affected children). The study sample consisted of 70 males (58.8%) and 49 females (41.2%). All of their hearing impairment levels were severe (71–95 dB) to profound (>95 dB); impairments were detected between 0 and 3 years old. All children had undergone cochlear implantation at Tokyo Medical University School of Medicine.

All cases underwent otoscopic examination and audiometric testing. Subjective tests of hearing acuity were assessed based on the auditory brain-stem response (ABR) and auditory steady-state response (ASSR) in infants and children. Behavioral observation audiometry (BOA) was used as a subsidiary measure to ABR and ASSR. A detailed history was taken to exclude other possible causes of deafness (such as neonatal complications, bacterial meningitis or other infections, use of ototoxic medication, or head trauma). Extended pedigrees were elicited from each family to exclude interfamilial relations. Temporal bone computed tomography was used in children to exclude any anomalies. The control group was carefully chosen to determine the carrier frequency, and consisted of 150 unrelated individuals with normal hearing.

Informed consent was obtained from the parents or guardians when necessary, and these were approved by the Ethical Committees of Juntendo University School of Medicine.

### 2.2. Genetic analysis

All samples from the children and normal controls were extracted from peripheral blood using the QIAamp DNA Blood Mini Kit (QIAGEN, Germantown, MD, USA). The coding region of *GJB2* was amplified from DNA samples by the polymerase chain reaction (PCR) using the primers *GJB2-F* 5'-GTGTGCATTCGCTTTTCCAG-3' and *GJB2-R* 5'-CGCAGTGCCTTGACA-3'. PCR products were sequenced using the PCR primers and sequence primers *GJB2-A* 5'-CCACGCCAGCGCTCCTAGTG-3' and *GJB2-B* 5'-GAAGATGCTGCTGCTGTGTAGG-3'. The sequencing reaction products were electrophoresed on an ABI Prism 310 Analyzer (Applied Biosystems). When no mutation or a single heterozygous mutation in *GJB2* was confirmed, we performed the multiplex PCR assay and direct sequencing for the coding region of *GJB6*. Multiplex PCR was carried out according to the method of Del Castillo et al. [24] to confirm the presence of the del(*GJB6*-D13S1830) and del(*GJB6*-D13S1854) deletions in *GJB6*.

Samples with no mutation or a single heterozygous mutation in *GJB2* and *GJB6* were analyzed for the gene dosage using real-time quantitative PCR (qPCR) to detect exon rearrangements in *GJB2* and *GJB6*. qPCR was performed with TaqMan Gene Expression Assays (Hs00269615\_s1 for *GJB2*, and Hs00272726\_s1 for *GJB6*, Applied Biosystems) and the 7500 Fast Real-Time PCR System (Applied Biosystems).

We obtained blood samples from the family which had one of two unreported mutations, pP225L, and the unreported one was confirmed as follows. The samples were subjected to mutation screening by PCR and direct sequencing for *GJB2*. The PCR product was subcloned into pCR 2.1 vector-TOPO by TOPO TA cloning (Invitrogen, Carlsbad, CA, USA), and independent subclones were sequenced employing M13forward (5'-TTGTAAAACGACGGCCAG) and reverse (5'-ACACAGGAAACAGCTATG) primers. The sequence data using in this study have been submitted to the GenBank

databases under accession numbers X65361, AB098335, NM\_000816, and NM\_001037.

### 2.3. Statistical analysis

A Z-test was used to calculate the difference in the allele frequency. In all statistical analyses, *P*-values of 0.01 or less were considered significant.

## 3. Results

### 3.1. Mutation screening of *GJB2*

*GJB2* mutations were found in 45 of the 119 affected individuals, and, of these, 35 patients were homozygous or compound heterozygous (29.4%). *GJB2*-related deafness patients, who had two *GJB2* mutant alleles, were found in 7 of 12 familial cases (58.3%), and there were 28 of 107 sporadic cases (26.2%). Eight mutations, including two unreported ones (p.R32S and p.P225L), were identified in these patients (Table 1). Three mutations were truncating mutations [one was a nonsense mutation (p.Y136X), and two were frameshifts (c.235delC and c.176-191del)]. The remaining five were missense mutations (p.R143W, p.G45E, p.T86R, p.R32S, and p.P225L). Among these mutations, c.235delC was the most frequent. The c.235delC mutation accounted for 52.9% (37 of 70) of the *GJB2*-mutated alleles (Table 1).

We identified 10 subjects who had three or more mutations. All of them had p.G45E and p.Y136X, including one homozygous child. TA cloning and sequencing of subcloned PCR products revealed that all subjects had both mutations in the same allele (data not shown). G45E accompanied with Y136X has been reported as a pathogenic mutation in previous reports, especially in Japanese patients [11,25], although it remains unclear which mutation is more related to the pathogenicity.

We compared the allele frequency for each mutation with that in Ohtsuka's study [25] (Fig. 1). The frequency of c.235delC and three mutations (p.R143W, p.G45E/Y136X, and c.176-191del) in this study were significantly different from that in Ohtsuka's study (*P* < 0.01). While the p.V37I mutation was reported to be the second most frequent autosomal recessive deafness allele in Asian countries [11,12], the present subjects did not follow this pattern.

In one subject, we identified a missense mutation, p.P225L, which has not previously been reported (Fig. 2). The sister and father of the proband had this mutation, while they showed a normal hearing function. The mother, with a normal hearing function, showed no mutation at this site, while she revealed only heterozygous p.G45E/Y136X mutation as a known pathogenic mutation of *GJB2*. The sequencing results of TA cloning further confirmed the existence of the pP225L nonsense mutation in this patient. We also identified another unreported mutation, p.R32S, in another subject. The patient had p.R32S/p.G45E/Y136X mutations. The amino acid positions of two unreported mutations

**Table 1**

Mutations identified in the *Cx26* gene, *GJB2* (NG\_008358.1), in child cases of congenital deafness.

Nucleotide change	Amino acid change	Allele (%)
c.235delC	p.Leu79CysfsX3	37 (52.9)
c.427C>T	p.Arg143Trp(p.R143W)	15 (21.4)
c.134G>A/c.408C>A	p.Gly45Glu/p.Tyr136X(p.G45E/Y136X)	10 (14.3)
c.176_191del	p.Gly59AlafsX18	4 (5.7)
c.257C>G	p.Thr86Arg(p.T86R)	2 (2.9)
c.94C>A	p.Arg32Ser <sup>a</sup> (p.R32S)	1 (1.4)
c.674C>T	p.Pro225Leu <sup>a</sup> (p.P225L)	1 (1.4)
Total mutations		70 (100)

<sup>a</sup> Novel mutations detected in this study.

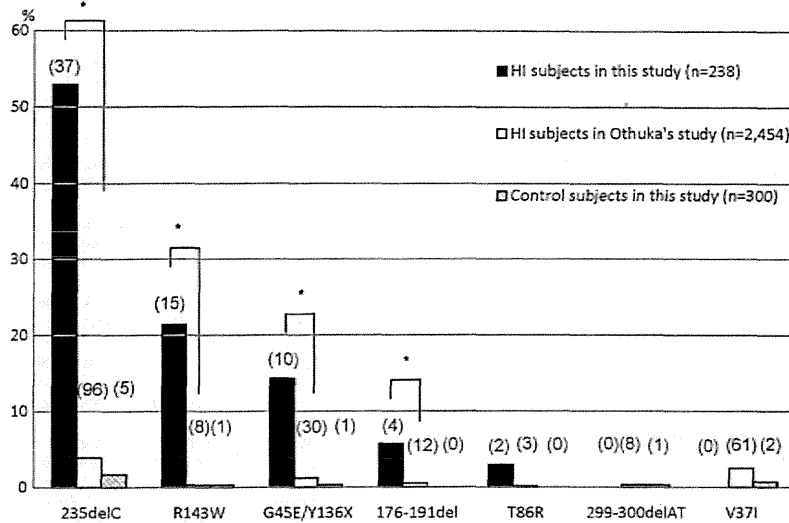


**Fig. 1.** Allele frequency for each mutation in three groups. A Z-test was used to assess the difference in frequency. Note the P-value of <0.01 between the two deafness groups for c.235delC, p.R143W, p.G45E/Y136X, and c.176-191del. \*P < 0.01.

(p.R32S and p.P225L) are highly conserved among various species, and we did not detect any of these mutations in 300 chromosomes in normal Japanese controls.

**4. Discussion**

In this study, *GJB2*-related deafness patients accounted for 29.4% of non-syndromic deafness cases. This frequency was less than in a previous report, which pointed to a frequency of around 50% [6]. Familial cases were twice as prevalent as sporadic cases. In most of the previously reported studies, the prevalence of *GJB2* mutations was significantly higher in familial non-syndromic deafness than in sporadic cases [7,26,27]. The frequent mutations of *GJB2* (c.235delC, p.R143W, p. G45E/Y136X, and c.176-191del) in this study were partly different from previous reports [25]. It is assumed that all of our subjects had severe to profound deafness,

as they had received cochlear implants, whereas Ohtsuka's subjects had mild to profound deafness and included heterozygous mutations. A few studies have confirmed that some genotypes are correlated with clinical phenotypes in *GJB2*-related deafness. Further, truncating mutations are associated with a greater degree of deafness than non-truncating mutations [9,21,22]. For this reason, three of these cases might be truncating mutations. In contrast, p.R143W mutation was previously implicated in an extraordinarily high prevalence of profound deafness in Ghana [15,28] and Caucasians [9]. This missense mutation may also show an important correlation with severe deafness in Japan. On the other hand, an effect of geography on the allele frequency may have been present, because most of our subjects were from a different area compared to a previous report [25].

The relation between p.V37I mutation of *GJB2* and SNHL is controversial. While some reports suggest that this mutation is

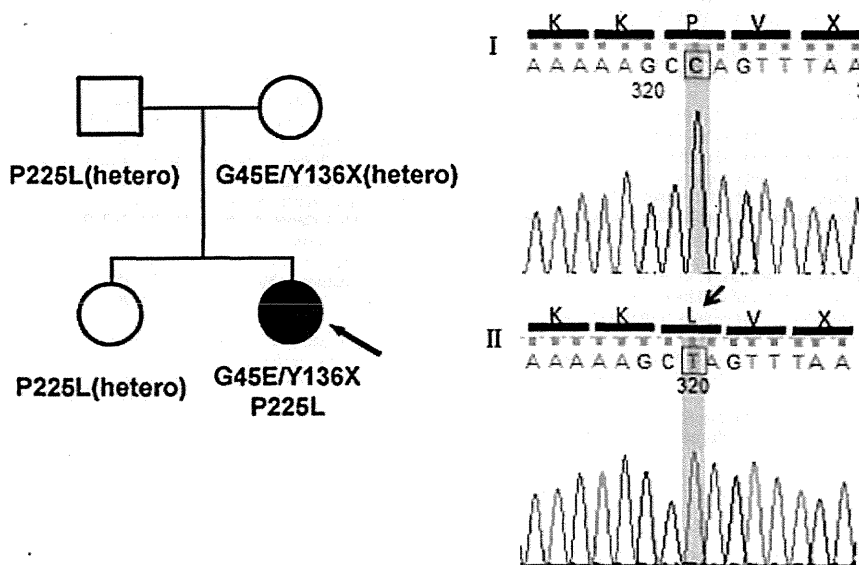


**Fig. 2.** (A) The pedigree and PCR direct sequencing results for the family; the arrow indicates the proband. (B) The sequencing results on TA cloning. Genomic PCR products were subcloned into a plasmid vector and sequenced separately (see Section 2). The sequences from independent clones are shown in the above two examples. I shows wild-type sequence, whereas II shows mutated sequence in which the proline residue is changed to leucine. Three of 8 subclones showed a missense mutation similar to that in II.

more common among individuals of Asian ancestry [11,12,29], others suggest that homozygous p.V371 is associated with slight/mild hearing loss [22,30,31]. In this study, no cases of homozygous p.V371 were observed. These findings support that this mutation is associated with mild hearing loss, because all of our subjects showed severe deafness.

The two unreported *GJB2* mutations, p.R32S and p.P225L, were not detected in normal hearing controls. These appeared in amino acid residues that were highly conserved. Additionally, three types of mutation were seen in arginine as the thirty-second amino acid, such as p.R32C, p.R32L, and p.R32H. Therefore, R32 is thought to be a mutation "hot spot." Thus, it is likely that these are pathological mutations, rather than rare or functionally neutral polymorphic changes. On the other hand, the mutation site of p.P225 located at the C-terminus of Connexin26 has not previously been reported. As the C-terminus region of connexins is thought to be an important region for intracellular molecular signaling and interaction with scaffolding proteins and the cytoskeleton [32–34], p.P225L mutation found in this study may affect important intracellular molecular networks to maintain the normal function of the cochlear gap junction.

## 5. Conclusion

In conclusion, this study identified significant genotypic features of Japanese children with profound non-syndromic deafness. Further research is required covering a broader range of genes in the subjects in this study with either single heterozygous or no mutation, in order to better understand the epidemiology of deafness in Japan.

## Acknowledgements

We thank all the subjects who participated in the present study. We also thank Ms. Naoko Tamura and Ms. Tomoko Kataoka (Tokyo Medical University School of Medicine), for recruiting families with non-syndromic deafness, and Ms. Junko Onoda (Juntendo University School of Medicine) for assisting in our experiments.

## References

- [1] A.C. Davis, The prevalence of deafness and reported hearing disability among adults in Great Britain, *Int. J. Epidemiol.* 18 (1989) 911–917.
- [2] D.H. Wilson, P.G. Walsh, L. Sanchez, The epidemiology of deafness in an Australian adult population, *Int. J. Epidemiol.* 28 (1999) 247–252.
- [3] N.E. Morton, Genetic epidemiology of deafness, *Ann. N. Y. Acad. Sci.* 630 (1991) 1631.
- [4] M.L. Marazita, L.M. Ploughman, B. Rawlings, E. Remington, K.S. Arnos, W.E. Nance, Genetic epidemiological studies of early-onset deafness in the U.S. school-age population, *Am. J. Med. Genet.* 46 (1993) 486–491.
- [5] V. Kalatzis, C. Petit, The fundamental and medical impacts of recent progress in research on hereditary hearing loss, *Hum. Mol. Genet.* 7 (1998) 1589–1597.
- [6] A. Kenneson, K. Van Naarden Braun, C. Boyle, *GJB2* (connexin 26) variants and nonsyndromic sensorineural hearing loss: a HuGE review, *Genet. Med.* 4 (2002) 258–274.
- [7] F. Denoyelle, S. Marlin, D. Weil, L. Moatti, P. Chauvin, E.N. Garabedian, et al., Clinical features of the prevalent form of childhood deafness, DFNB1, due to a connexin-26 gene defect: Implications for genetic counselling, *Lancet* 353 (1999) 1298–1303.
- [8] A. Murgia, E. Orzan, R. Polli, M. Martella, C. Vinanzi, E. Leonardi, et al., Cx26 deafness: mutation analysis and clinical variability, *J. Med. Genet.* 36 (1999) 829–832.
- [9] R.L. Snoeckx, P.L. Huygen, D. Feldmann, S. Marlin, F. Denoyelle, J. Waligora, et al., *GJB2* mutations and degree of hearing loss: a multicenter study, *Am. J. Hum. Genet.* 77 (2005) 945–957.
- [10] Y. Fuse, K. Doi, T. Hasegawa, A. Sugii, H. Hibino, T. Kubo, Three novel connexin26 gene mutations in autosomal recessive non-syndromic deafness, *Neuro Report* 10 (1999) 1853–1857.
- [11] S. Abe, S. Usami, H. Shinkawa, P.M. Kelley, W.J. Kimberling, Prevalent connexin 26 gene (*GJB2*) mutations in Japanese, *J. Med. Genet.* 37 (2000) 41–43.
- [12] T. Kudo, K. Ikeda, S. Kure, Y. Matsubara, T. Oshima, K. Watanabe, et al., Novel mutations in the connexin 26 gene (*GJB2*) responsible for childhood deafness in the Japanese population, *Am. J. Med. Genet.* 90 (2000) 141–145.
- [13] H.J. Park, S.H. Hahn, Y.M. Chun, K. Park, H.N. Kim, Connexin 26 mutations associated with nonsyndromic hearing loss, *Laryngoscope* 110 (2000) 1535–1538.
- [14] P. Gasparini, R. Rabionet, G. Barbutani, S. Melchionda, M. Petersen, K. Brondum-Nielsen, et al., High carrier frequency of the 35delG deafness mutation in European populations, Genetic Analysis Consortium of *GJB2* 35delG, *Eur. J. Hum. Genet.* 8 (2000) 19–23.
- [15] G.W. Brobby, B. Muller-Myhsok, R.D. Horstmann, Connexin 26 R143W mutation associated with recessive nonsyndromic sensorineural deafness in Africa, *N. Engl. J. Med.* 338 (1998) 548–550.
- [16] M. Maheshwari, R. Vijaya, M. Ghosh, S. Shastri, M. Kabra, P.S. Menon, Screening of families with autosomal recessive non-syndromic hearing impairment (ARNSHI) for mutations in *GJB2* gene: Indian scenario, *Am. J. Med. Genet. A* 120A (2003) 180–184.
- [17] M. RamShankar, S. Girirajan, O. Dagan, H.M. Ravi Shankar, R. Jalvi, R. Rangasayee, et al., Contribution of connexin26 (*GJB2*) mutations and founder effect to non-syndromic hearing loss in India, *J. Med. Genet.* 40 (2003) e68.
- [18] G. Minářik, V. Ferák, E. Feráková, A. Fieck, H. Poláková, L. Kádasi, High frequency of *GJB2* mutation W24X among Slovak Romany (Gypsy) patients with non-syndromic hearing loss (NSHL), *Gen. Physiol. Biophys.* 22 (2003) 549–556.
- [19] P. Seeman, M. Malíková, D. Rasková, O. Bendová, D. Groh, M. Kubáková, et al., Spectrum and frequencies of mutations in the *GJB2* (Cx26) gene among 156 Czech patients with pre-lingual deafness, *Clin. Genet.* 66 (2004) 152–157.
- [20] A. Alvarez, I. del Castillo, M. Villamar, L.A. Aguirre, A. González-Neira, A. López-Nevot, et al., High prevalence of the W24X mutation in the gene encoding connexin-26 (*GJB2*) in Spanish Romani (gypsies) with autosomal recessive non-syndromic hearing loss, *Am. J. Med. Genet. A* 137A (2005) 255–258.
- [21] K. Cryns, E. Orzan, A. Murgia, P.L. Huygen, F. Moreno, I. del Castillo, et al., A genotype-phenotype correlation for *GJB2* (connexin 26) deafness, *J. Med. Genet.* 41 (2004) 147–154.
- [22] T. Oguchi, A. Ohtsuka, S. Hashimoto, A. Oshima, S. Abe, Y. Kobayashi, et al., Clinical features of patients with *GJB2* (connexin 26) mutations: Severity of hearing loss is correlated with genotypes and protein expression patterns, *J. Hum. Genet.* 50 (2005) 76–83.
- [23] K. Fukushima, K. Sugata, N. Kasai, S. Fukuda, R. Nagayasu, N. Toida, et al., Better speech performance in cochlear implant patients with *GJB2*-related deafness, *Int. J. Pediatr. Otorhinolaryngol.* 62 (2002) 151–157.
- [24] F.J. Del Castillo, M. Rodríguez-Ballesteros, A. Alvarez, T. Hutchin, E. Leonardi, C.A. de Oliveira, et al., A novel deletion involving the connexin-30 gene, *del(GJB6-d13s1854)*, found in trans with mutations in the *GJB2* gene (connexin-26) in subjects with DFNB1 non-syndromic deafness, *J. Med. Genet.* 42 (2005) 588–594.
- [25] A. Ohtsuka, I. Yuge, S. Kimura, A. Namba, S. Abe, L. Van Laer, et al., *GJB2* deafness gene shows a specific spectrum of mutations in Japan, including a frequent founder mutation, *Hum. Genet.* 112 (2003) 329–333.
- [26] J. Löffler, D. Neĭahm, A. Hirst-Stadlmann, B. Gunther, H.J. Menzel, G. Utermann, et al., Sensorineural hearing loss and the incidence of Cx26 mutations in Austria, *Eur. J. Hum. Genet.* 9 (2001) 226–230.
- [27] A. Pampanos, J. Economides, V. Iliadou, P. Neou, P. Leotsakos, N. Voyiatzis, et al., Prevalence of *GJB2* mutations in prelingual deafness in the Greek population, *Int. J. Pediatr. Otorhinolaryngol.* 65 (2002) 101–108.
- [28] C. Hamelmann, G.K. Amedofu, K. Albrecht, B. Muntau, A. Gelhaus, G.W. Brobby, et al., Pattern of connexin 26 (*GJB2*) mutations causing sensorineural deafness in Ghana, *Hum. Mutat.* 18 (2001) 84–85.
- [29] WangYC, C.Y. Kung, M.C. Su, C.C. Su, H.M. Hsu, C.C. Tsai, et al., Mutations of Cx26 gene (*GJB2*) for prelingual deafness in Taiwan, *Eur. J. Hum. Genet.* 10 (2002) 495–498.
- [30] C. Huculak, H. Bruyere, T.N. Nelson, F.K. Kozak, S. Langlois, V371 connexin 26 allele in patients with sensorineural hearing loss: Evidence of its pathogenicity, *Am. J. Med. Genet. A* 140 (2006) 2394–2400.
- [31] H.H. Dahl, K. Saunders, T.M. Kelly, A.H. Osborn, S. Wilcox, B. Cone-Wesson, et al., Prevalence and nature of connexin 26 mutations in children with non-syndromic deafness, *Med. J. Aust.* 175 (2001) 191–194.
- [32] L.A. Elias, D.D. Wang, A.R. Kriegstein, Gap junction adhesion is necessary for radial migration in the neocortex, *Nature* 448 (2007) 901–907.
- [33] P.E. Martin, G. Blundell, S. Ahmad, R.J. Errington, W.H. Evans, Multiple pathways in the trafficking and assembly of connexin 26, 32 and 43 into gap junction intercellular communication channels, *J. Cell Sci.* 114 (2001) 3845–3855.
- [34] K.A. Schalper, N. Palacios-Prado, M.A. Retamal, K.F. Shoji, A.D. Martínez, J.C. Sáez, Connexin hemichannel composition determines the FGF-1-induced membrane permeability and free  $[Ca^{2+}]_i$  responses, *Mol. Biol. Cell* 19 (2008) 3501–3513.

## III. 臨床応用の進歩

多能性幹細胞を用いた遺伝性難聴に対する  
内耳細胞治療法の開発

神谷和作 池田勝久

Inner ear cell therapy for hereditary deafness with multipotent stem cells

Kazusaku Kamiya, Katsuhisa Ikeda

Department of Otorhinolaryngology, Juntendo University School of Medicine

## Abstract

Congenital deafness affects about 1 in 1,000 children and the half of them have genetic background such as connexin26 gene mutation. The strategy to rescue such hereditary deafness has not been developed yet. Inner ear cell therapy for hereditary deafness has been studied using some laboratory animals and multipotent stem cells, although the successful reports for the hearing recovery accompanied with supplementation of the normal functional cells followed by tissue repair and recovery of the cellular/molecular functions have been still few. To succeed in hearing recovery by inner ear cell therapy, appropriate cell type, surgical approach and the stem cell homing system to the niche are thought to be required.

**Key words:** hereditary deafness, mesenchymal stem cell, inner ear, cochlea, connexin26

## はじめに

先天性難聴は1,000出生に1人と高頻度に発症し聴覚・言語発育障害の極めて高度なQOLの低下をもたらすが、その半数以上は遺伝性と考えられている。遺伝性難聴の原因遺伝子は代表的なコネキシン26遺伝子(connexin26, Cx26, GJB2)をはじめとして多くが同定されている。しかしその根本的治療法は皆無であり、近年では再生医療の遺伝性難聴への応用が大きく期待されている。著者らは蝸牛線維細胞を標的とした感音性難聴モデルへの内耳細胞治療法に成功し、幹細胞導入により感音性難聴の聴力回復が可能であることを実証した<sup>1)</sup>。一方でヒト遺伝

性難聴の臨床症状に近いとされる遺伝子改変モデルマウスの開発も進めてきた。ヒト非症候性難聴DFN3モデルBrn4欠損マウス(Brn4KO)は遺伝性難聴の遺伝子改変モデルの先駆けとして報告され、蝸牛線維細胞の変性とそれに伴う内リンパ電位(endocochlear potential: EP)と呼ばれる内耳特異的な電位形成のシステムに異常が生じることが初めて発見された(図1)<sup>2)</sup>。更に世界で最も高頻度に変異が検出される代表的な難聴遺伝子、コネキシン26(Cx26)遺伝子(GJB2)の優性阻害変異型トランスジェニック(Tg)マウス(Cx26Tg)<sup>3)</sup>の作製によっても、高頻度に発生する遺伝性難聴に対する分子病態が明らかになってきた。このマウスは生後発達期に

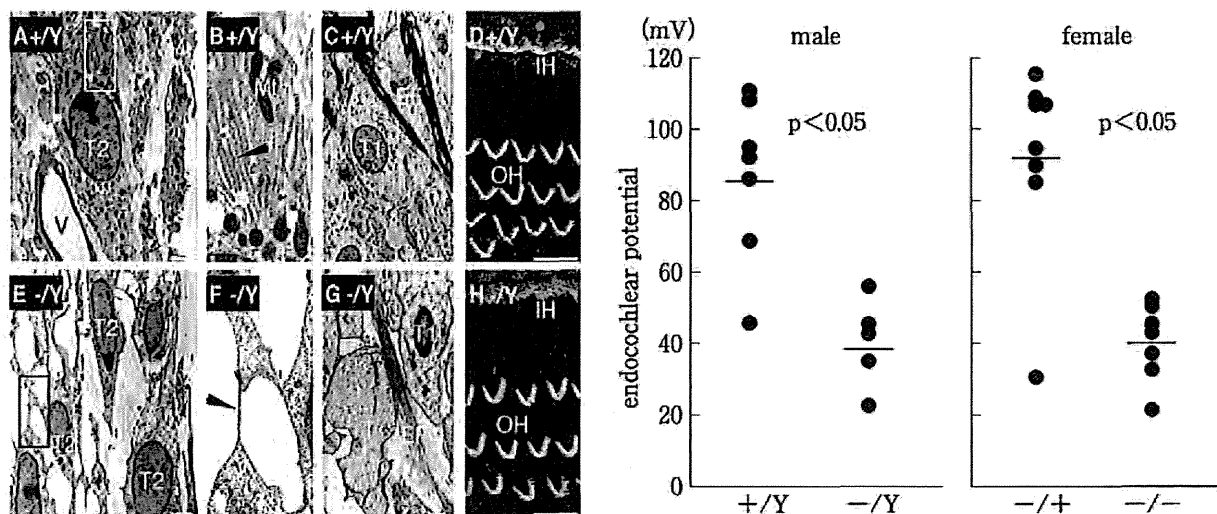


図1 ヒト遺伝性難聴モデル Brn4 遺伝子欠損マウスにおける  
蝸牛線維細胞変性の発見(文献<sup>2)</sup>より引用)

蝸牛有毛細胞を含むコルチ器に変性がないにもかかわらず(H), 蝸牛線維細胞に変性がみられ(F, 矢頭), その結果蝸牛内リンパ電位が著しく低下する(右グラフ)。→すなわち蝸牛線維細胞を正常細胞に置換することができれば聴力が回復する可能性が非常に高い。

有毛細胞を含む感覚上皮領域であるコルチ器において, コルチトンネルやヌエル腔などの特殊細胞構築(cytoarchitecture)が正常に形成されないという病理的特徴があるが<sup>4)</sup>, 外有毛細胞を単離すると正常と同等の有毛細胞特有の運動能を示すことが明らかとなり<sup>5)</sup>, 残存した有毛細胞を活用した細胞治療により, 聴力回復の可能性が十分に考えられる。

著者らの研究チームでは Cx26 の内耳特異的欠損マウス(Cx26cKO)を新規開発し, 同モデルマウスによる更なる分子病態の解明とそれに応じた細胞治療法の開発を進めている。

### 1. 内耳細胞治療の必要性

遺伝性難聴では一部の患者に人工内耳の有用性も報告されているが, 本来の聴覚機能を回復させる根本的治療法はいまだ存在しない。遺伝性難聴の第一次的な原因細胞は有毛細胞以外にも蝸牛線維細胞や支持細胞などであることが明らかとなっている。この多様な異常変異細胞を修復するには, 新たな治療戦略として多能性幹細胞を用いた効率的細胞治療法の開発が必要であると考えられる。内耳再生医療の技術開発により, これまで補聴器や人工内耳などの適用で

根本的治療が存在しなかった遺伝性難聴患者の日常生活における負担は大幅に減り, 細胞が永続的に生着すればその後の手術や投薬の頻度が軽減し, 極めて現実的な高度医療への発展が期待できる。

### 2. 内耳への細胞治療とそのアプローチ

近年の内耳再生医療に関する基礎研究分野は, *in vitro*での有毛細胞への分化誘導においては年々進歩している。最近では *in vitro*においてマウス胚性幹(ES)細胞や人工多能性幹(iPS)細胞から聴毛を有する有毛細胞へ分化誘導することも可能となっており<sup>6)</sup>, 細胞工学的分野では大きな成果が得られている。しかしながらそれらの細胞を移植により内耳組織へ生着させ, 同時に機能的補足や組織修復によって聴力回復を誘導する細胞治療の試みは成功例が少なく, 引用度の高い論文での報告も少ない。聴力回復を目的とした内耳細胞治療法を開発するためには移植細胞の生着と機能発現を同時に考慮し, 内耳の解剖学的特徴および各細胞の生理学的特徴を十分に理解することが重要であると考えられる。

内耳は特殊なリンパ液で満たされた独特な構造をもち, 血液-脳関門と同様に「血液-内耳関

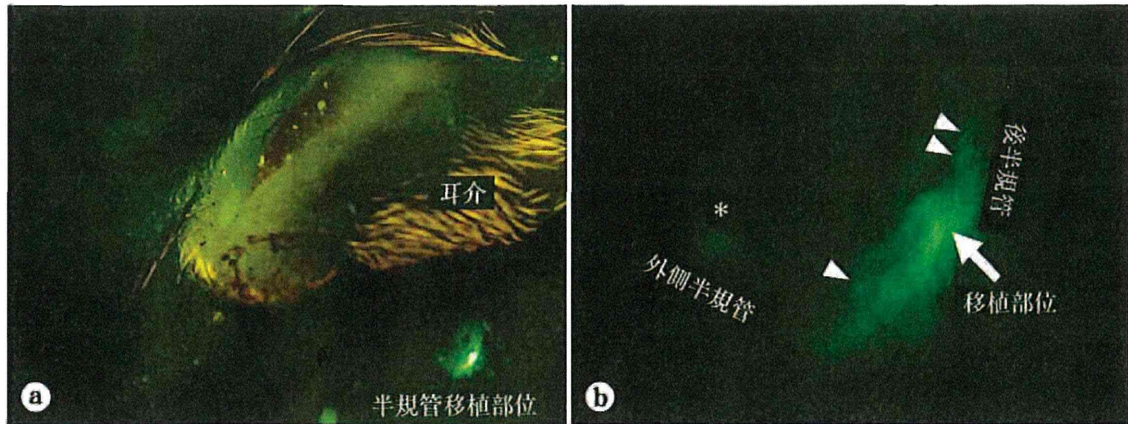


図2 マウスへの間葉系幹細胞移植2週間後の移植部蛍光実体顕微鏡像

- a. 耳後部切開により半規管を露出し、移植細胞塊が拒絶されずに生着していることを確認。  
 b. 更に移植部位より播種性に進展し、コロニーを形成(矢頭)。後半規管から外側半規管への移行も確認された(\*)。

門'と呼ばれる血管系を有するため内耳有毛細胞やその周辺細胞への薬物的アプローチが難しい。しかし移動能・多分化能を兼ね備えた幹細胞による内耳細胞治療の方法が確立すれば、難聴の根本的治療への有効なツールになると考えられる。

著者らの初期の検討実験では、蝸牛管付近より細胞液投与を試みた際はどの部位でも手術による永続的な聴力低下がみられ、蝸牛組織には線維化が認められた。著者らはIguchiらの方法<sup>7)</sup>を参考にラットの後半規管および外側半規管に小孔を開け<sup>7)</sup>、片側から微小チューブを挿入し細胞液の外リンパ腔還流( $1 \times 10^5$  cells/ $20 \mu\text{L} \times 10$  min)を行い、良好な結果が得られている。この方法では手術による聴力低下はほとんどみられず、大量の細胞を蝸牛内に導入することができるため、内耳細胞治療に適した投与方法であると思われる。著者らは細胞液環流後に骨髄間葉系幹細胞の細胞塊を半規管の小孔に挿入することにより、内液の漏出を防ぎ、細胞生着にも良好な結果を得ている(図2)。

### 3. *in vitro* での内耳有毛細胞作製法の開発

体外で未分化細胞より内耳有毛細胞を作製しようとする試みは数多く行われてきたが、*in vitro* において有毛細胞特異的マーカーを発現

させた報告はこれまで複数報告されてきた。それらを発展させ、遺伝子発現だけでなく特殊な巨大繊毛をもつ内耳有毛細胞に特殊形態を形成させ、最終的には音の振動を感知する機械的刺激受容チャネル(機械電気シグナル変換チャネル: mechano-electrical transduction (MET) channel)を併せ持つ細胞を作製させる試みがついで行われてきた。2007年にCorwinらの研究チームはニワトリの間葉系細胞から動毛、不動毛をもつ有毛細胞を作製した<sup>6)</sup>。次段階として、哺乳類細胞から有毛細胞を*in vitro*で作製する技術が期待されてきた。そして2010年、スタンフォード大学のOshima, Hellerらの研究チームによりマウスのES細胞およびiPS細胞から*in vitro*で内耳有毛細胞を作製する画期的技術が発表され、作製された細胞が音の振動を感知できる有毛細胞特有のMET機能を有することが明らかとなった<sup>8)</sup>。これにより内耳有毛細胞を体外で人工的に増殖・分化させることが可能であることが示された。この報告では、未分化細胞から内耳前駆細胞へ、段階的に分化を進めているため、これを応用すればすべての内耳構成細胞への分化能をもつ内耳細胞を*in vitro*にて作製し内耳移植に最適な細胞を選抜することが可能となる。同方法ではES/iPS細胞の浮遊培養後に接着培養を行い分化制御因子としてDkk1, SIS3, IGF-1の添加培養、その後の

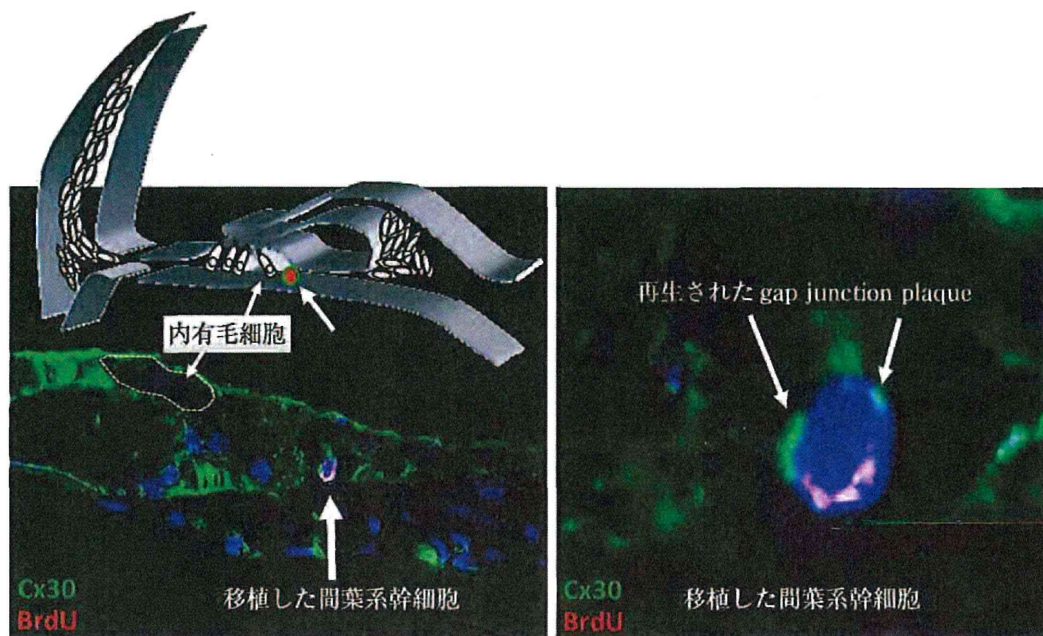


図3 移植した間葉系幹細胞において再生されたギャップ結合プラーク

半規管外リンパ液領域より移植され、コルチ器の内毛細胞近傍に侵入した間葉系幹細胞(左)。同細胞は蝸牛支持細胞の機能構造であるコネクシン複合体で構成されるギャップ結合プラークを形成している(右)。

bFGF 添加後に鶏杯卵形囊細胞との共培養を行うことで、動毛や機械電気シグナル変換が可能な不動毛をもつ内耳有毛細胞様細胞を得ることを可能としている。

#### 4. 蝸牛標的組織への幹細胞の誘導

前述のように体外で内耳細胞を作製する技術は大きく進展しているが、内耳細胞治療において、作製された細胞を蝸牛組織へ直接的に挿入することは蝸牛の構造上困難であり、適切な箇所に幹細胞を導入できる細胞誘導システムが必須であると考えられる。特に有毛細胞やその支持細胞および内リンパ液に接する血管糸細胞、蝸牛線維細胞など、適切な箇所に幹細胞を導入し、その微小環境(niche, ニッチ, ニッシェ)に応じて分化させることが必要である。そのためには適切な幹細胞ホーミング(標的組織へ遊走し微小環境に生着)の分子機構を理解し応用することが重要であると考えられる。

マックスプランク研究所の研究チームは、心筋虚血後に骨髄由来間葉系幹細胞が癒痕層へ効率的にホーミングされるには走化性因子 MCP1

とその受容体 CCR2 およびその下流において細胞遊走を制御している FROUNT による分子経路が重要な役割を担っていることを明らかにした<sup>9)</sup>。著者らの研究チームでは、実験的に誘発した蝸牛線維細胞損傷部においても MCP1 が高発現することを発見している(文献<sup>10)</sup>および未発表データ)。これを応用し CCR2 を共発現する骨髄間葉系幹細胞株を作製して内耳細胞治療実験に用いることで、良好な細胞誘導効果が得られている。これまで蝸牛線維細胞領域に軽度損傷を与えた難聴動物では蝸牛線維細胞に移植細胞が侵入しており、一部は有毛細胞の近傍の支持細胞領域に侵入し、同領域の主な機能構造であるギャップ結合プラークを形成した(図3)。

#### おわりに

将来的に内耳細胞治療への活用が期待できる細胞は、患者の骨髄より樹立可能な骨髄間葉系幹細胞、iPS細胞およびES細胞由来の内耳前駆細胞などであるが、これらの細胞と適切な幹細胞ホーミングの分子機構を応用し適切な遺伝性難聴モデル動物において方法を選抜することに



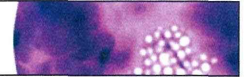
より、細胞を補うだけではなく遺伝子変異をもつ異常細胞を正常細胞に置換するという全く新しい観点での方法論を確立できる。この方法論の発展により、将来的には多様な遺伝性難聴患

者に対し薬物治療などとは異なる、組織損傷の種類と度合いに対応した低リスクで高い効果をもつ新規難聴治療法の開発が期待できる。

## ■ 文 献

---

- 1) Kamiya K, et al: Mesenchymal stem cell transplantation accelerates hearing recovery through the repair of injured cochlear fibrocytes. *Am J Pathol* 171: 214-226, 2007.
- 2) Minowa O, et al: Altered cochlear fibrocytes in a mouse model of DFN3 nonsyndromic deafness. *Science* 285: 1408-1411, 1999.
- 3) Kudo T, et al: Transgenic expression of a dominant-negative connexin26 causes degeneration of the organ of Corti and non-syndromic deafness. *Hum Mol Genet* 12: 995-1004, 2003.
- 4) Inoshita A, et al: Postnatal development of the organ of Corti in dominant-negative Gjb2 transgenic mice. *Neuroscience* 156: 1039-1047, 2008.
- 5) Minekawa A, et al: Cochlear outer hair cells in a dominant-negative connexin26 mutant mouse preserve non-linear capacitance in spite of impaired distortion product otoacoustic emission. *Neuroscience* 164: 1312-1319, 2009.
- 6) Hu Z, Corwin JT: Inner ear hair cells produced in vitro by a mesenchymal-to-epithelial transition. *Proc Natl Acad Sci USA* 104: 16675-16680, 2007.
- 7) Iguchi F, et al: Surgical techniques for cell transplantation into the mouse cochlea. *Acta Otolaryngol Suppl* (551): 43-47, 2004.
- 8) Oshima K, et al: Mechanosensitive hair cell-like cells from embryonic and induced pluripotent stem cells. *Cell* 141: 704-716, 2010.
- 9) Belema-Bedada F, et al: Efficient homing of multipotent adult mesenchymal stem cells depends on FROUNT-mediated clustering of CCR2. *Cell Stem Cell* 2: 566-575, 2008.



## ORIGINAL ARTICLE

# Analysis of subcellular localization of Myo7a, Pcdh15 and Sans in *Ush1c* knockout mice

Denise Yan<sup>1</sup>, Kazusaku Kamiya<sup>1</sup>, Xiao Mei Ouyang and Xue Zhong Liu

Department of Otolaryngology, University of Miami, Miami, FL, USA

INTERNATIONAL  
JOURNAL OF  
EXPERIMENTAL  
PATHOLOGY

## Summary

Usher syndrome (USH) is the most frequent cause of combined deaf-blindness in man. An important finding from mouse models and molecular studies is that the USH proteins are integrated into a protein network that regulates inner ear morphogenesis. To understand further the function of harmonin in the pathogenesis of USH1, we have generated a targeted null mutation *Ush1c* mouse model. Here, we examine the effects of null mutation of the *Ush1c* gene on subcellular localization of Myo7a, Pcdh15 and Sans in the inner ear. Morphology and proteins distributions were analysed in cochlear sections and whole mount preparations from *Ush1c*<sup>-/-</sup> and *Ush1c*<sup>+/-</sup> controls mice. We observed the same distribution of Myo7a throughout the cytoplasm in knockout and control mice. However, we detected Pcdh15 at the base of stereocilia and in the cuticular plate in cochlear hair cells from *Ush1c*<sup>+/-</sup> controls, whereas in the knockout *Ush1c*<sup>-/-</sup> mice, Pcdh15 staining was concentrated in the apical region of the outer hair cells and no defined staining was detected at the base of stereocilia nor in the cuticular plate. We showed localization of Sans in the stereocilia of controls mouse cochlear hair cells. However, in cochleae from *Ush1c*<sup>-/-</sup> mice, strong Sans signals were detected towards the base of stereocilia close to their insertion point into the cuticular plate. Our data indicate that the disassembly of the USH1 network caused by absence of harmonin may have led to the mis-localization of the Protocadherin 15 and Sans proteins in the cochlear hair cells of *Ush1c*<sup>-/-</sup> knockout mice.

## Keywords

deafness, inner ear, knockout mouse, Usher 1C, Usher syndrome

doi: 10.1111/j.1365-2613.2010.00751.x

Received for publication:

30 June 2010

Accepted for publication:

21 October 2010

## Correspondence:

Dr Xue Zhong Liu

Department of Otolaryngology (D-48)

University of Miami

1666 NW 12th Avenue

Miami, FL 33136

USA

Tel.: 305 243 5695

Fax: 305 243 4925

E-mail: xliu@med.miami.edu

<sup>1</sup>These authors contributed equally to this work.

## Introduction

Usher syndrome (USH) is an autosomal recessive disorder characterized by congenital hearing loss and progressive retinal degradation leading to gradual loss of the visual field and blindness.

Three major clinical subtypes (USH type I, USH type II and USH type III) are distinguished on the basis of differences in the severity of the hearing loss, the presence or absence of vestibular dysfunction and the age of onset of retinitis pigmentosa (RP) (Smith *et al.* 1994). In USH type 1, the hearing loss is profound and vestibular function is absent. The onset of progressive RP is before puberty. Usher syndrome type 2 is associated with less severe deafness, normal vestibular function and onset of RP during or after puberty. Usher syndrome type 3 patients also have milder

deafness, but, unlike in USH2, the hearing loss is progressive, there is variable impairment of vestibular function and late-onset RP. Each USH subtype is genetically heterogeneous. To date, seven USH1 loci (USH1B-USH1H) have been identified by linkage analyses of USH1 families. Five of the corresponding genes have been cloned: the actin-based motor protein myosin VIIa (*Myo7a*, *USH1B*) (Gibson *et al.* 1995; Weil *et al.* 1995); two cadherin-related proteins, otocadherin or Cadherin 23 (*Cdh23*, *USH1D*) (Bolz *et al.* 2001; Bork *et al.* 2001) and Protocadherin 15 (*Pcdh15*, *USH1F*) (Ahmed *et al.* 2001; Alagramam *et al.* 2001a); and two scaffold proteins, harmonin (*USH1C*) (Verpy *et al.* 2000; Bitner-Glindzicz *et al.* 2000) and Sans (*USH1G*) (Kikkawa *et al.* 2003; Weil *et al.* 2003). The USH proteins are involved in hair bundle morphogenesis in the inner ear by means of protein-protein interactions. In a combination of cell cotransfection

and *in vitro* binding assays, harmonin has been shown to bind to any of the other USH proteins (El-Amraoui & Petit 2005; Yan & Liu 2010; Zheng et al. 2010).

A mouse mutant has been reported for each of the known *Ush1* genes; shaker1 (*sh1*) for *Myo7a* (Gibson et al. 1995), waltzer (*v*) for *Cdh23* (Di Palma et al. 2001; Wilson et al. 2001), Ames waltzer (*av*) for *Pcdh15* (Alagramam et al. 2001b), deaf circler (*dscr*) and targeted mouse models for *Ush1c* (Johnson et al. 2003; Lentz et al. 2007; Lefevre et al. 2008; Tian et al. 2010) and Jackson shaker (*js*) for *Ush1g* (Kikkawa et al. 2003). All of these mice are deaf, exhibit vestibular dysfunction and display similar morphological abnormalities in hair bundle development. In all of these models, the hair cell stereocilia vary irregularly in height and splay out from one another indicating defective lateral interactions. Investigations into the localization of the USH proteins within the developing stereocilia in mice, combined with *in vitro* studies to determine the various interactions between the constituent molecules, have revealed an 'Usher interactome' that is responsible for bundle cohesion. Some of the *Ush1* mutant mice (*sh1*, *v*, *av*) exhibited electroretinogram anomalies (Libby & Steel 2001), a defective retinal pigment epithelium has been described in *sh1* mice (Gibbs et al. 2003, 2004) and retinal degeneration has been reported in *Ush1c216AA* knock-in mice (Lentz et al. 2010).

The gene encoding harmonin consists of 28 coding exons, alternative splicing of which leads to 10 USH1C isoforms. These alternative transcripts form three subclasses (a, b and c) depending on the domain composition of the protein. The isoform 'a' transcript subclass is expressed ubiquitously in many tissues, whereas the longest 'b' transcript is restricted largely to the inner ear. The short isoform 'c' has a much broader tissue distribution. The harmonin isoforms differ in the number of protein-protein interaction domains (PDZ, postsynaptic density/disc-large/zonal occludens 1), coiled-coiled domains (CC) and the presence of a proline-serine-threonine-rich domain (Verpy et al. 2000). Deaf circler, *dscr* and *dscr-2J* spontaneous mutant mice have been described as models for human *USH1C*. The mutant *dscr* is defective in all harmonin isoforms (a, b and c). Only the harmonin b isoform subclass is affected by the *dscr-2J* mutation (Johnson et al. 2003). However, altered harmonin isoforms may retain partial function because the normal reading frame of the *Ush1c* transcripts is not changed in the shortened *dscr* transcripts of either isoform a or isoform b. Furthermore, none of the three PDZ-encoding domains are deleted in *dscr* mutant transcripts. Both a *USH1C* knockin and knockout mouse have also been reported (Lentz et al. 2007; Lefevre et al. 2008). To further understand the role of harmonin in the pathogenesis that leads to USH1, we have recently generated a targeted null mutation *Ush1c* mouse model in which the first four exons of the *Usher 1c* gene have been replaced by a reporter gene (Liu et al. 2005; Yan et al. 2006; Tian et al. 2010). Our model is unique because none of the previous targeted mouse models for *USH1C* include a reporter gene in the construct to facilitate expression analysis in various tissues. Here, we examine the effects of *Ush1c*

mutation on spatial subcellular localization of *Myo7a*, *Pcdh15* and *Sans* proteins in the inner ear. In whole mount of inner ears from mutant, *Myo7a* was not affected at the timepoint we analysed the mutant mice, although it is a critical part of the USH interactome. However, we found both *Pcdh15* and *Sans* displayed an altered localization in the mutant mice that may have resulted from disruption of the entire USH1 complex.

## Materials and methods

Inner ears isolated from the *Ush1c*<sup>-/-</sup> and *Ush1c*<sup>+/-</sup> mice at postnatal day 21 (PD21) were fixed by immersion in 4% paraformaldehyde (pH 7.4) for 2-5 h at 4°C. The organ of Corti was dissected from the cochlear spiral in phosphate-buffered saline (PBS) using a fine needle. Samples were then permeabilized in 0.5% Triton X-100 for 30 min, then washed in PBS. Non-specific binding sites were blocked using 5% normal goat serum (Life Technologies, Gaithersburg, MD, USA) and 2% bovine serum albumin (ICN, Aurora, OH, USA) in PBS for 2 h. Samples were incubated for 2 h in the primary antibodies at 5 µg/ml in blocking solution. After several rinses in PBS, samples were incubated in Alexa Fluor 488-conjugated anti-rabbit IgG goat at 1:400 (Molecular Probes, Eugene, OR, USA) for 40 min. Samples were mounted using a ProLong Antifade kit (Molecular Probes) and analysed with a laser scanning confocal microscope (LSM-510; Zeiss, Thornwood, NY, USA). The polyclonal antibody against *Myo7a* (ab3481) was obtained from Abcam (Cambridge, MA, USA). The anti-PCDH15 antibody was generated against a mixed peptide sequence corresponding to amino acid 24-37 (SWGQYDDDWQYEDC) and amino acid 1847-1860 (C+TFTTQPPASNPQWG), and the anti-USH1G antibody was against the central portion of the *Sans* protein (amino acid 354-372).

## Results

Homozygous mutant mice (*Ush1c*<sup>-/-</sup>) exhibit the abnormal behaviour (circling and/head-tossing) that are typical of mice with profound hearing loss and vestibular dysfunction. *Ush1c*<sup>-/-</sup> mice were completely deaf, as there was no detectable auditory-evoked brainstem response (ABR) with 100 dB SPL stimuli, whereas age-matched *Ush1c*<sup>+/-</sup> controls showed ABR thresholds in the normal hearing-range at PD15 and PD22. Examination of hair cell surface preparations by scanning electron microscopy from birth (PD0) to PD120 in *Ush1c*<sup>-/-</sup> showed progressively disorganized outer hair cell (OHC) stereocilia compared with the well-organized pattern and rigid structure typical of normal stereocilia. Stereocilia of inner hair cells (IHCs) of mutant mice also exhibited a disorganized appearance, but to a lesser degree than did the OHCs (Tian et al. 2010).

To address the possibility that absence of harmonin disrupts the USH1 protein complex, we analysed in this study the distribution of Myosin VIIa protein in whole mounts, and of Protocadherin 15 and *Sans* in cross sections, of inner

ears from *Ush1c*<sup>-/-</sup> mice. Light microscopy examinations of sections through apical regions of the cochleae of *Ush1c*<sup>-/-</sup> at PD21 revealed no apparent hair cell degeneration (data not shown). However, in cochlear whole mounts from *Ush1c*<sup>-/-</sup> mice at PD21, some gaps are seen in the regular array of hair cells. Although the single row of IHCs and the three rows of OHCs can be distinguished by surface scanning of the hair cells (Figure 1b), fragmentation of the OHC stereociliary bundles into two clumps was observed, instead of an integral, single 'V'-shaped bundle as in wild-type hair cells (Figure 1d, arrow). This fragmented aspect was not detected in stereocilia of IHCs at this timepoint (IHC; Figure 1b), suggesting that they were beginning to degenerate. However, confocal microscopic analysis of the hair cells in the basal

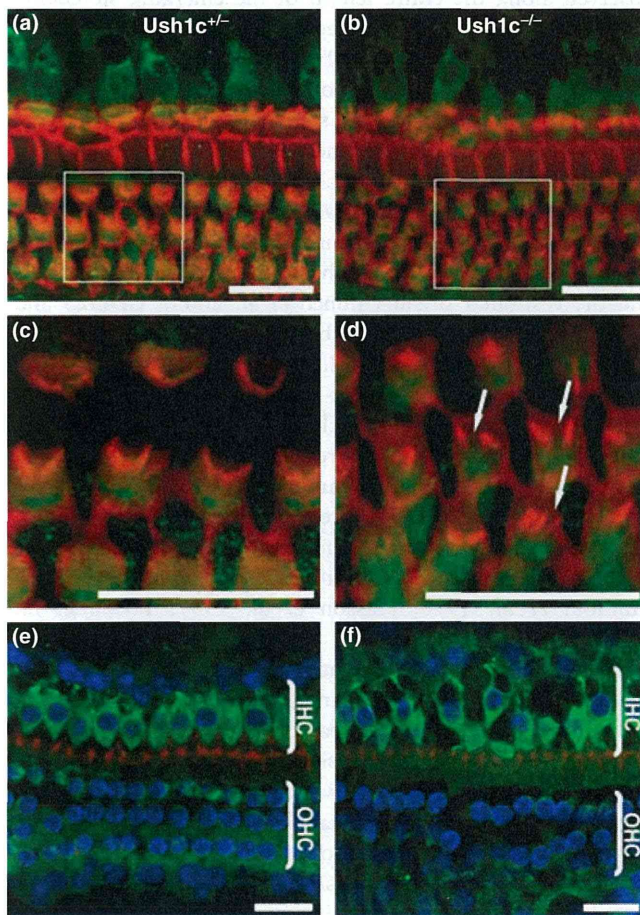


**Figure 1** Abnormalities at the apical surface of outer hair cells (OHC) and structural defects of the hair cells in *Ush1c*<sup>-/-</sup> mice at PD21. Cochlear whole mounts were stained with phalloidin (red) to reveal F-actin in stereocilia and an antibody against myosin 7a (green) to show the basal structure of the hair cells in *Ush1c*<sup>+/-</sup> (a, c and e) and *Ush1c*<sup>-/-</sup> mice (b, d and f). Stereocilia defects were observed in the middle part of the stereocilia bundles of the OHCs (d, arrows) that were not detected in stereocilia of inner hair cells (IHC; b). c and d show magnified images corresponding to the boxed areas in a and b respectively. The confocal analysis at the basal level of hair cells with nuclear staining (e and f) (DAPI, Blue). Bars = 20  $\mu$ m.

layer revealed structural morphological abnormalities in both OHCs and IHCs, with a more disorganized appearance in IHC (Figure 1f). Scanning electron microscopy of *Ush1c*<sup>-/-</sup> mice from PD21 to PD120 showed a progressive degeneration of the hair cells and stereocilia of the cochlea (Tian *et al.* 2010). Myosin 7a has previously been shown to be expressed within the stereocilia and within the cuticular plate, which anchors the base of each stereocilium. In the present study, Myosin 7a was distributed throughout the cytoplasm in *Ush1c*<sup>-/-</sup> and control mice in the labelled hair cells, revealing structural morphological abnormalities characterized by disorganized, misaligned inner and OHCs (Figure 1e, f).

In cochlear hair cells from heterozygous *Ush1c*<sup>+/-</sup> control mice, we detected Protocadherin 15 at the base of stereocilia and in the cuticular plate (as shown by the arrow in Figure 2c), whereas in the mutant *Ush1c*<sup>-/-</sup>, Protocadherin 15 immunoreactivity was found accumulated in the apical region of the OHC and no defined staining was detected at the base of stereocilia and little Pcdh15 expression was present at the cuticular plate (Figure 2d). Likewise, in the knockout mice, Sans was undetectable in the stereocilia bundles of cochlear hair cells at PD21 (Figures 3b, d), in contrast to the heterozygous controls (*Ush1c*<sup>+/-</sup>, Figure 3c). Instead, strong Sans staining was observed towards the base of stereocilia close to their insertion point into the cuticular plate with a slight staining of the cytoplasmic region of OHC in cochleae from *Ush1c*<sup>-/-</sup> mice (Figure 3d). These results suggest a mis-localization of the Pcdh15 and Sans proteins in

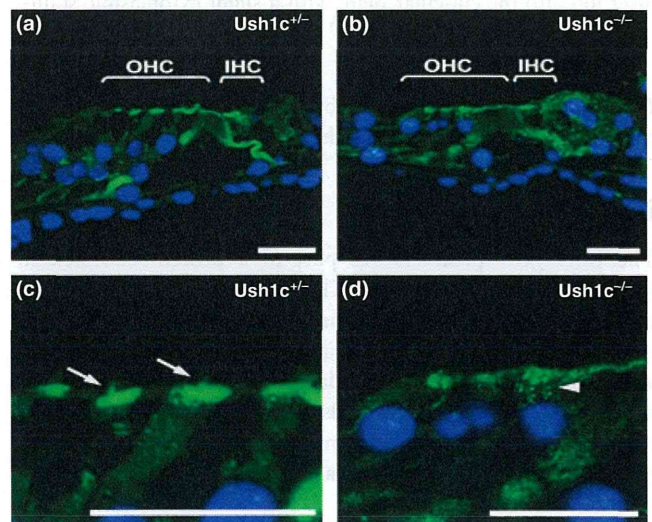


**Figure 2** Localization of Protocadherin 15 (green) in the cochlear hair cells of *Ush1c*-knockout mice at PD21. Cross sections of the organ of Corti were stained with an antibody to Protocadherin 15 (green). In *Ush1c*<sup>+/-</sup> mice (a and c), expression of Protocadherin 15 was localized at the base of stereocilia (left panel, arrow) and in the cuticular plate. In contrast, in *Ush1c*<sup>-/-</sup> mice (b and d), Protocadherin 15 immunoreactivity appears (arrowhead) diffuse above nuclei (DAPI-Blue). Bars = 20  $\mu$ m.